# Microfabricated PMN-PT on Silicon cantilevers with improved static and dynamic piezoelectric actuation: development, characterization and control.

Ioan Alexandru Ivan, *Member, IEEE,* Joel Agnus, Micky Rakotondrabe, *Member, IEEE,* and Philippe Lutz, *Member, IEEE,* Nicolas Chaillet, *Member IEEE*

***Abstract*— The paper reports a new composite bimorph Piezo-MEMS actuator based on the mono-crystalline and high piezoelectric coefficient material PMN-PT. The technology is based on the gold bonding of two bulk materials (PMN-PT and Silicon) followed by the Deep Reactive Ion Etching (DRIE) on the silicon side, leading to an optimized displacement actuator. The process requires an external re-polarization, yet the piezoelectric properties are conserved. The device is characterized then modeled and operated in a closed-loop control. The actuation capabilities results are compared to the ones of a classical PZT-ceramic actuator of equivalent size, demonstrating a 3 to 4 times net gain in terms of displacement range. The dynamics are improved by a factor of 2.5X for the same actuating range. The newly microfabricated actuator is also lighter and compatible with the silicon batch fabrication. Applications panel include microrobotics, microassembly, cells and gene manipulation etc.**

## I. Introduction

Relaxor based ferroelectric single crystals like PMN-PT and PZN-PT has been grown and investigated starting late nineties. First sensors, ultrasonic transducers and bending actuators were soon developed. Nowadays the trend is towards further miniaturization and silicon-integrated devices [1], which are also known as Piezo-MEMS. Single crystal PMN-PT materials show some important advantages [2] with respect to the classical PZT ceramics: extremely high and anisotropic piezoelectric constants and coupling factors, reduced ferroelectric nonlinearities, low losses, crystalline structure, cryogenic operation. Drawbacks refer to a certain mechanical fragility, low coercitive field and low Curie temperature, high cost.

The purpose of this work is in the design, development, characterisation and control of a first basic cantilevered structure of bulk PMN-PT on a Silicon substrate exploiting a custom thermocompressive bonding technique and the dry etching of the Silicon side, in order to achieve an optimum displacement actuator.

Only few very recent papers document devices exploiting the bonding of piezoelectric and silicon wavers. J. Peng et al. [3] recently presented the first micromachined PMN PT ultrasonic transducer pPMUT. E. Aktakka et al. [4] also developed ultrasonic diaphragms of PZT on silicon substrates. The present paper shows a separate technology developed in parallel for the first micromachined PMN-PT / Silicon cantilevers. Potential applications include microrobotics, micromanipulation, microassembly, atomic force microscopy, biological samples manipulation etc.

The paper is divided as follows: Section II presents the basics of the cantilevered actuators and the PMN-PT material, referencing to our previous ref. [5]. Then it establishes the actuator specifications and shows the microtechnology flowchart. Section III is dedicated to extensive static and dynamic characterisation of the developed actuators, in a constant comparison with classical PZT actuators. Section IV shows an example of displacement closed-loop control of the newly designed actuators and, finally, the section Conclusions briefly concludes the paper.

## II. Design and development

### *A. Modelling and Design Specifications*

Our previous papers [5][6] already documented the properties of the PMN-PT and the related considerations for the design of bending actuators. The piezoelectric-on-a passive-material cantilevers are also called in the literature composite bimorph or unimorph piezoelectric actuators.

As well known, the maximum free displacement of a composite piezo cantilever varies with the square of its length and is relatively independent of its width. For a given piezoelectric wafer, there exists an optimum passive material thickness, which primarily depends on the ratio of the stiffness coefficients. There are tradeoffs in the design of such actuators, as higher lengths will privilege coarse displacement ranges yet less blocking force, while higher thicknesses will provide increased stiffness and dynamics with the cost of reduced ranges.

The design criteria for these first prototypes of PMN-PT-on-Silicon actuators to be ever built were suited for tasks

This work was supported by the EU FP7-SP3-People Program under Grant No: PIEF-GA-2008-219412 (New Micro-Robotic Systems featuring Piezoelectric Adaptive MicroStructures for Sensing and Actuating, with Associated Embedded Control: MicroPAdS).

Authors are with the UFC/ENSMMM/ FEMTO-ST Institute, AS2M Department, 24 Rue Alain Savary, 25000 Besancon, France (phone: +33-381-402-803; fax: +333-381-853-998; e-mail: {alex.ivan, nicolas.chaillet, mrakoton, , plutz}@ femto-st.fr, joel.agnus@ens2m.fr).

such as microrobotics, microassembly and bio cells manipulation. The considered micromanipulated object varies from a few micrometers up to several hundred micrometers, where the maximum required force should be of a few mN (very often less). The actuating range should be of several hundred micrometers, or ideally as high as possible. After several analytical and FEM analysis we defined the following design criteria:

- ✓ The thickness of PMN-PT material is fixed, of 200µm.
- ✓ The optimum related silicon thickness is 60µm; however, for validation reasons, we chose to develop a panel four different Si thickness: 25µm, 50µm, 75µm and 100µm.
- ✓ Three widths were considered, progressively smaller for technological reasons: 700µm, 500µm and 300µm.
- ✓ The active length varied between 6 and 13 mm
- ✓ A solid silicon base was planned to properly clamp the actuator.

*B. The Piezoelectric Materials*

The PMN-PT plates were growth by TRS Technologies under the codes X2B and X2C. The piezoelectric and compliance tensors used for modelling the devices were entered however from the ref [7] documenting the same cut <001> and a relatively close concentration (30%PT). The PMN-PT manufacturers do not provide the complete coefficients probably also due to the broad parameter dispersion between different lots, reaching easily ±30%.

For comparative reasons, and for emphasising the state-of-the-art performance of the PMN-PT actuators, we manufactured in parallel some "classical" actuator beams, made of PZT ceramics glued on Nickel plates. These plates were cut at the same sizes as the PMN-PT plates. The material was PIC151 from PI, a soft ceramic similar to the PZT-5H.

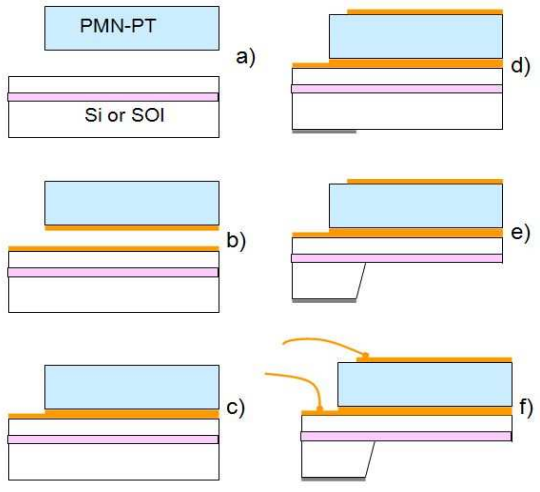


Figure 1. Microactuator's flowchart: a) initial PMN-PT and Silicon wafers; b) Cr-Au sputtering at interface; c) Gold bonding; d) top electrode (Cr-Au) and bottom mask (Cr-Al) sputtering; e) saw dicing into individual beams followed by DRIE; f) wire bonding and external poling.

In the figures to come (for the coloured printed version) we will use a colour convention: red for PZT and bluish for PMN-PT. Two different PMN-PT lots were used for manufacturing the actuators; they will be identified by two slightly different blue tones.

*C. The PMN-PT/Si Micro-actuators flowchart*

The technology is based on the following steps:

**i)** The PMN-PT and Silicon wafers are lapped and cleaned.

**ii)** Gold sputtering on a Chrome adhesion buffer at interface of both PMN-PT and Silicon – see Fig. 1.b. Gold thickness: 350 nm. Progressive process, to limit the stress build-up.

**iii)** Thermo-compression bonding of the Au layers using an EVG machine; bonding is performed in 10mbar vacuum, at 2 MPa and 60°C. Bonding time: ~10 hours. For proper surfaces the bonding quality is insured. Some destructive tests may be done like for instance the one in Fig. 2. The bulk material should not crack at the gold bonding interface.

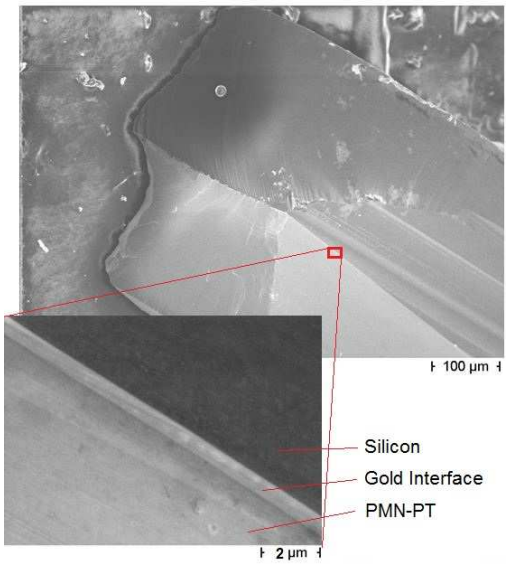


Figure 2. A scanning electron microscope image of a destructive test on a PMN-PT/Si beam, the fracturing direction shows a very good soldering quality. The 0.7 µm gold interface remain intact.

**iv)** Top Chrome-Gold electrode deposition using a hard mask or photolithography followed by wet etch. Lift-off is equally possible. Gold layer is ~100 nm thick.

**v)** Bottom Chrome-Aluminium DRIE-mask deposition using a hard mask, photolithography or lift-off process (Fig1.d).

**vi)** Saw dicing of the wafer into individual beams which will look like in Fig 3. Dicing is performed before DRIE as because of the beams fragility.

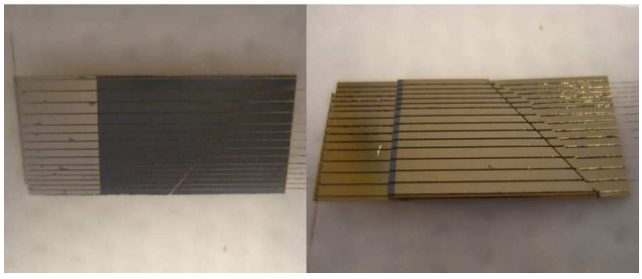

Figure 3. An array of PMN-PT cantilevers diced and ready for the silicon etching step. Bottom side (left) and top side (right) photos.

**vii)** DRIE etching of the bottom silicon side. In the Fig 1.e the silicon wafer is of SOI (silicon-on-insulator) type which has the advantage of a stopping barer to a fixed thickness. We used instead a simple Silicon wafer and managed the etching times to reach the appropriate thicknesses ($h_{Si}$ = 25, 50, 75 and 100 µm). Figures 4 and 5 show the results.

**viii)** Conductive paste or gold wire bonding connection as in Fig. 1.f and Fig. 4 right.

**ix)** Final external re-poling of the PMN-PT material at room temperature and a constant 10 kV/cm field for over 10 minutes.

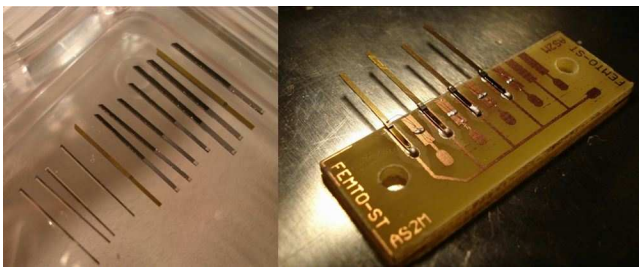


Figure 4. PMN-PT on Silicon cantilevers of various widths and thicknesses, after DRIE (left) and after the final wire bonding (right).

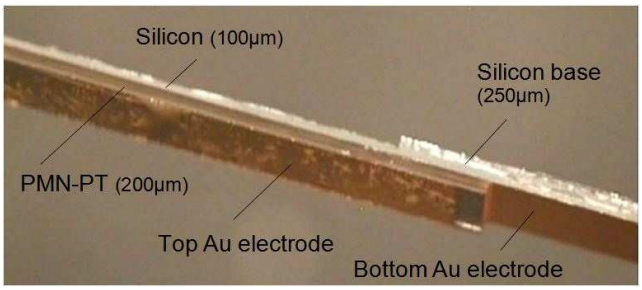


Figure 5. Close-up image of a final PMN-PT / Si actuator.

## III. CHARACTERIZATION

Extensive experiments have been performed to characterize the actuation behavior and its nonlinearities. We recall that the beams had four different thicknesses (25, 50, 75, 100 µm), three different widths (0.3, 0.5 and 0.7 mm), two different material lots and various lengths. The position of the laser spot point was set eventually constant in all static experiments, corresponding to an active beam of 9.3 mm, having thus a common measurement base.

### *A. PMN-PT Material Re-Poling*

The material has to be re-poled due to the high pressure withstood during bonding and due to high temperature during DRIE. Re-poling of the PMN-PT material in both positive and negative field is reversible. Figures 6 and 7 show the typical polarisation shapes, which are rather different corresponding to the two material lots (X2B and X2C) that were discussed before. The curves were recorded in a low frequency high voltage sinue waveform (+/- 200V, 3mHz or 700s).

The first conclusion is that the piezoelectric strain vs. the external field (aka the“butterfly” curves) is not symmetrical, for reasons that have to be further investigated. The net stroke is higher in the original positive polarization, especially for the material lot in Fig.6. As for the figure 7, the net stroke is similar in both directions, the hysteresis being however significantly higher in negative direction.

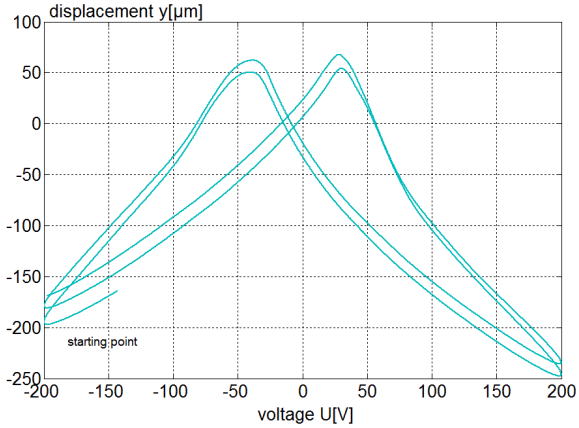


Figure 6. External re-poling curve of a PMN-PT/Si actuator ($h_{Si}$ = 100µm, $h_{PMN\text{-}PT}$ = 200µm, $w$=0.7mm, $L$=9.3mm). Frequency is set 0.003 Hz

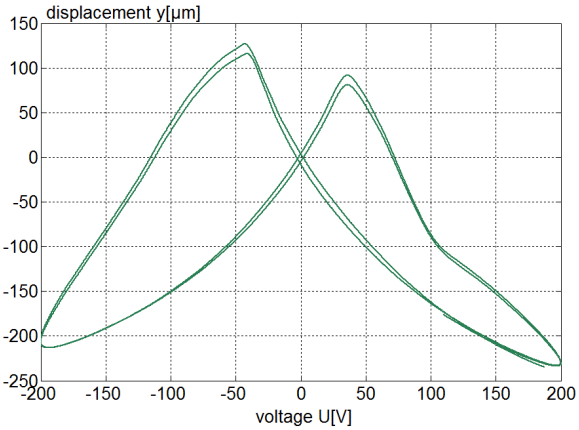


Figure 6. External re-poling curve of a PMN-PT/Si actuator ($h_{Si}$ = 75µm, $h_{PMN\text{-}PT}$ = 200µm, $w$=0.7mm, $L$=9.3mm). Frequency is set 0.003 Hz

As expected, the coercitive field of the PMN-PT is quite low compared to PZT, of -43V or 2.15 kV/cm which prevents large negative signal operation as in the case of PZT.

### *B. COMSOL Simulations*

The simulations details are not provided here, but were already depicted in the previous paper [5]. The differences between the analytical and finite elements (FEM) results were also presented in [6]. Due to the lack of manufacturers' data, the TRS material PMN-PT was modeled with the coefficients taken from [7] while the PZT PIC151 with the PZT-5H embedded in COMSOL.

The simulation curves from Fig. 8 simulated for a beam of 9.3 mm long show that the passive material (Si, Ni) thicknesses for an optimal actuation are:

- 65µm of Si for a 200µm layer of PMN-30PT
- 75µm of Ni for a 200µm layer of PZT-5H

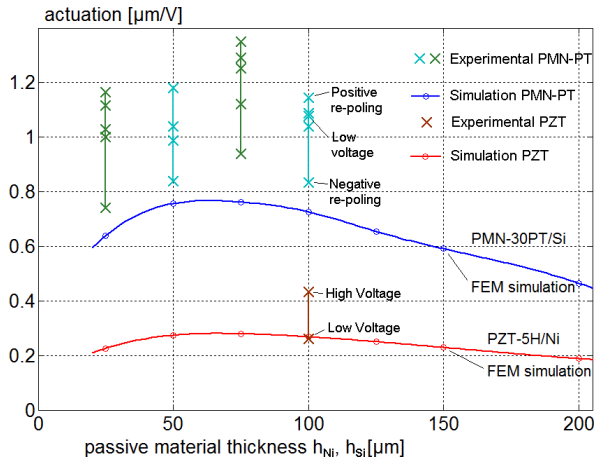


Figure 8. Experimental and FEM simulation results of PMN-PT/Si and PZT/Ni actuators. The beams are $w$=0.7 mm wide, $L$=9.3 mm long (active area) and the piezoelectric layer is $h_{PMN\text{-}PT}$=200 µm. The experimental actuation of the PMN-PT is even higher than the predicted simulations.

### C. Actuation characteristics

The experimental results of the four types of PMN-PT / Si actuators as well as the PZT / Ni used as a comparison are confronted with the simulation results in the same Fig. 8. The vertical plots show the dispersion values between different beams, at large and small voltages, either positive or negative.

The experimental and the modelled PZT actuator results are in a very good agreement. At low voltage the experimental point superposes the simulation curve. For a 200V value the PZT actuation is significantly higher, as expected.

As for the PMN-PT family, we notice that the experimental points are unexpectedly higher than the simulations, certainly due to the difference between the actual material coefficients and the parameters simulated from [7]. The difference is by roughly +50% in the positive way but, as discussed, they may be probably explained by the different material stoichiometry. More accurate simulations should be performed after measuring and identifying the exact piezoelectric, compliance and dielectric matrices.

Some of the experimental curves are plotted in the Fig. 9 – 14 and the related values are centralised in the Table 1.

The 25 µm and 75 µm actuators belong from a single PMN-PT material lot while the 50 µm and 100 µm actuators

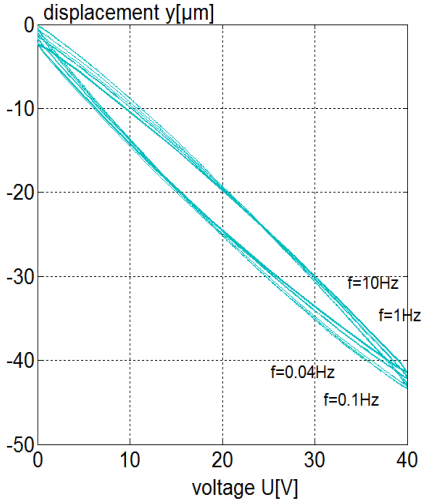


Fig. 9. "Low" voltage hysteresis PMN-PT ($h_{Si}$ = 100µm, $h_{PMN\text{-}PT}$ = 200µm, $L$=9.3mm)

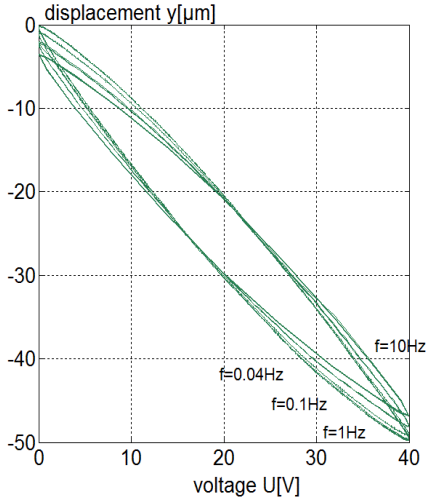


Fig. 10. "Low" voltage hysteresis PMN-PT ($h_{Si}$ = 75µm, $h_{PMN\text{-}PT}$ = 200µm, $L$=9.3mm)

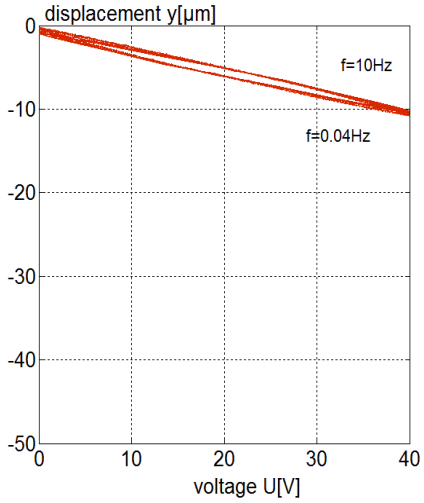


Fig. 11. "Low" voltage hysteresis PZT ($h_{Ni}$ = 100µm, $h_{PZT}$ = 200µm, $L$=9.3mm)

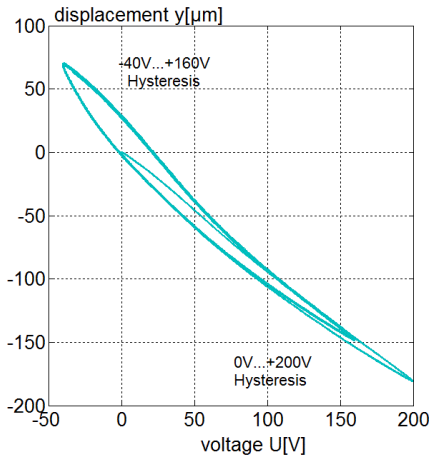


Fig. 12. High voltage hysteresis - PMN-PT ($h_{Si}$ = 100µm, $h_{PMN\text{-}PT}$ = 200µm, $L$=9.3mm)

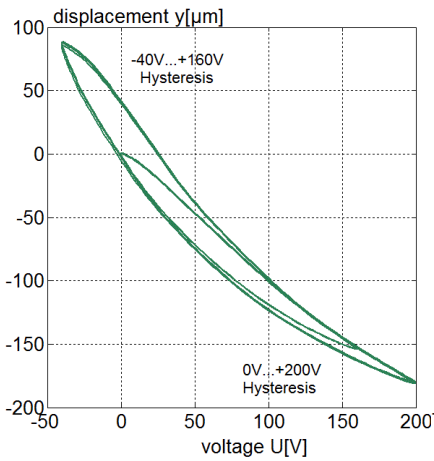


Fig. 13. High voltage hysteresis - PMN-PT ($h_{Si}$ = 25µm, $h_{PMN\text{-}PT}$ = 200µm, $L$=9.3mm)

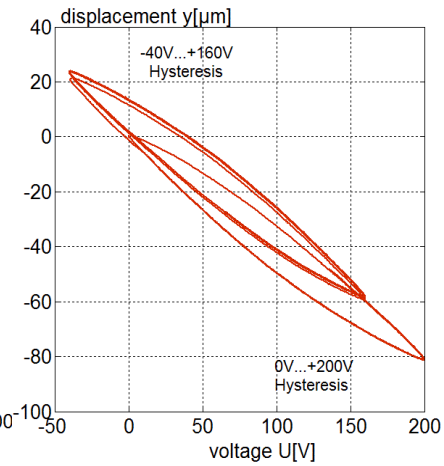


Fig. 14. High voltage hysteresis PZT ($h_{Ni}$ = 100µm, $h_{PZT}$ = 200µm, $L$=9.3mm)

belong from another PMN-PT lot with slightly lower piezoelectric properties.

### *D. Nonlinear Properties*

Piezoelectric materials typify the hysteresis and creep nonlinearities. The influence of these phenomena generally increased with the amplitude of the applied electric field. In this part, we characterize the small and large signal hysteresis of the developed PMN-PT/Si piezo-cantilevers.

First, the small signal hysteresis of two PMN-PT cantilevers (belonging to the two lots) are compared with the PZT/Ni beam. By small signal we mean voltages that provide symmetric shapes, like up to 40V. For that, a sine input $U$ is applied of fixed amplitude and varying frequency, then the output $y$ is reported and finally the curve $(U,y)$ is plotted for each. The data is presented in Table 1 and some plots are shown for illustration. As we can see in the Fig. 9-11 that are rendered at the same scale, the PMN-PT/Si performs a large stroke with an associated hysteresis of 12.8% and 18% respectively, compared to the PZT which is at 9.5%.

The next experiment consists in applying some large voltage (200V) low frequency signals, the results being pictured in Fig. 12-14. In the case of PZT we notice an increased actuation with the voltage but with the cost of a much higher hysteresis. The PMN-PT hysteresis is significantly lower for large positive values but nonlinear; from 50V we notice how the saturation starts occurring. As for the reverse fields, hysteresis shape is very large and asymmetric (Fig. 12-13) The material may be driven theoretically until 400V but with the cost of an even increased nonlinear behavior.

### *E. Dynamics*

Piezoelectric devices are particularly recognized for their large variety of bandwidth, according firstly to the structure developed and secondly to the type of piezoelectric material. To evaluate the comparative performances for the three piezocantilevers, a frequency analysis was carried out. Fig. 15 pictures the resulting magnitudes.

In order to make a comparison with the nonlinerities of classic piezocantilevers (PZT/Ni), the following actuators were experimented:

1) a new PMN-PT/Si cantilever developed in this paper, with dimensions: $L$=11mm (spot at $L$=10mm), $w$=0.7mm, $h_{total}$=0.275mm ($h_{PMN\text{-}PT}$=0.2mm and $h_{Si}$=0.075mm);

1) a classic PZT/Ni piezocantilever having the same length as the developed PMN-PT/Si one (spot $L$=10mm, $w$=0.7mm, $h_{total}$ =0.300mm, $h_{Ni}$=0.1mm));

2) and another classic PZT/Ni piezocantilever that can perform the same range of output deflection $y$[µm] for the same range of input voltage $U$[V] than the developed PMN-PT/Si. For that, while their widths and the thicknesses remain the same ($w$=1mm, $h_{total}$=0.275mm), the length of the PZT/Ni is $L$=17.5mm (spot at L=17mm) in order to attain the expected deflection.

First, it is again confirmed that, for the same dimensions, PZT/Ni piezocantilevers show lower gains than the PMN-PT/Si in low frequency due to the smaller $d_{31}$ piezoelectric coefficient.

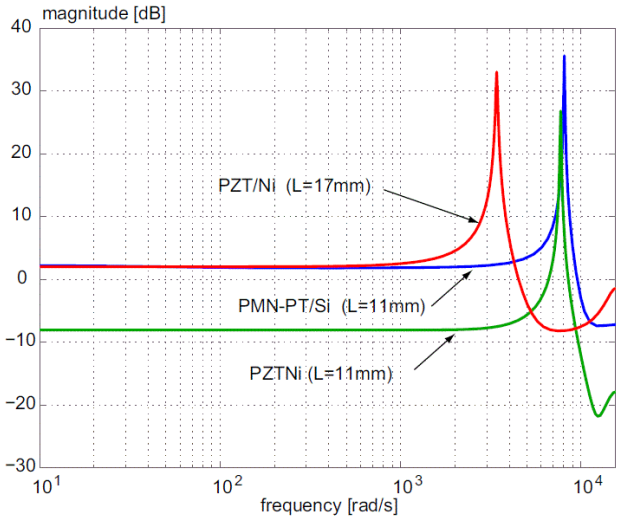


Fig. 15. Experimental magnitude of a PMN-PT piezocantilever compared to the magnitudes of two PZT piezocantilevers (same size / same static gain). Exact sizes are provided in Section III.E.

We also remark that, for the same length, their resonant peaks (1209Hz, 1260Hz) are quite similar despite material compliance differences. PMN-PT is more compliant that the PZT but the resonant frequency is in the same range due to the larger thickness and density of Ni relative to the one of Si. As for the 17mm PZT/Ni actuator that can perform the same static gain as the 11mm PMN-PT/Si, the corresponding bandwidth of PZT is significantly lower (517Hz), due to the its larger beam length. Overall, the damping factor of all cantilevers is comparable.

TABLE I. STATIC ACTUATION PERFORMANCE OF PMN-PT/SI AND PZT/NI BENDING ACTUATORS. THE LENGTH IS CONSIDERED 9.3 MM.

| Actuator Type | Small signal (≤40V) Average displacement and hysteresis | | Large signal (0 to + or -200V) Min/Max displacement and hysteresis | | Voltage Range |
|---|---|---|---|---|---|
| | µm/V | % | µm/V | % | V |
| PMN-PT / Si | | | | | |
| #1: 200µm/100µm | 1.07 | 12.8% | 0.83 – 1.15 | 8.3-13.7% | -44…+400V or -400…+44V |
| #2: 200µm/75µm | 1.25 | 18% | 0.95 – 1.35 | 13.9-17.7% | |
| #3: 200µm/50µm | 0.97 | 17% | 0.83 – 1.18 | 11-13.2% | |
| #4: 200µm/25µm | 1.02 | 28% | 0.75 – 1.16 | 12-21,7% | |
| PZT / Ni | | | | | |
| #5 :200µm/100µm | 0.26 | 9.5% | 0.38 – 0.43 | 15-17% | -150…+300V |

## IV. Modeling and Control

In this part, we design a controller for one of the PMN-PT/Si piezocantilevers (the one presented in Section III.E). Indeed, despite the high resolution of piezoelectric materials in general, hysteresis and creep nonlinearities lead to the loss of accuracy. Furthermore, resonance peaks are often unwanted for several applications such as in micromanipulation and microassembly. They can provoke an unstability of the manipulated or positioned micro-objects.

### *A. Modeling*

To model the piezocantilever, we follow the procedure proposed in [8]. In this, a creeped, hysteretic and oscillating piezoactuator can be approximated by a linear model where the creep is considered as an output disturbance to be rejected and the hysteresis and the dynamics are a linear time invariant model with uncertainty. If too strong, this uncertainty may be used for the controller synthesis. We have:

$$y = KD(s) + d \qquad (1)$$

Where $K$ is the static gain identified approximately from a hysteresis curve similar like the one in Fig. 10, $D(s)$ is the dynamic part identified from Fig. 15, and $d$ is an output disturbance that contains other disturbances (creep, thermal drift etc.). After identification, we obtain:

$$G(s) = KD(s) = \frac{1.283}{1.58\times10^{-8}s^2 + 2.57\times10^{-6}s + 1} \qquad (2)$$

Notice that, in order to have a passive system, the $U$ voltage sign is physically reversed such that, unlike until now, a positive sign displacement is attained upon applying a positive voltage.

### *B. Direct synthesis of a controller*

Let Fig.16 be the scheme of the closed-loop, where $y_r$ is the reference input and $C(s)$ is the controller to be designed.

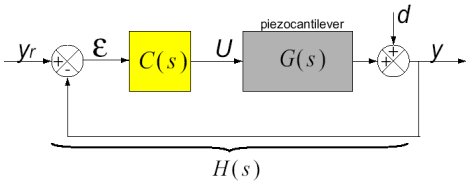


Fig. 16. Block-scheme of the closed-loop.

The main obhtly jective is to find the $C(s)$ controller such that the piezocantilever perform certain specified performances. For that, if $H(s)$ denotes the closed-loop with $d$=0, we have: $H(s) = \frac{CG}{1+CG}$. If $H(s)$ is imposed through specifications, we can derive the controller ([9]):

$$C(s) = \frac{1}{G}\cdot\frac{H}{(1-H)} \qquad (3)$$

The reliability conditions of the controller are: $G(s)$ must be stable and $H(s)$ is chosen such than $C(s)$ is proper (causal).

### *C. Specifications*

The specifications imposed to the closed-loop are:

- the static error tends towards zero;
- the settling time is less than 40ms;
- and the overshoot is null.

From these specifications, it appears that a 1st order of $H(s)$ is sufficient, such as $H(s) = \frac{1}{1+0.013s}$. However, in order to respect the causality of $C(s)$, $H(s)$ must be at least of a second order. We therefore choose:

$$H(s) = \frac{1}{(1+0.013s)\left(1+\frac{0.013}{5}s\right)} \qquad (4)$$

Finally, the resulting controller from (3) and (4) is:

$$C(s) = \frac{346\times10^{-6}\left(s^2+162s+6.3\times10^7\right)}{s(s+450)} \qquad (5)$$

### *D. Experimental results*

The controller (5) has been implemented in Matlab-Simulink on a dSPACE real-time board. The sampling time is 0.2ms. A series of reference step inputs $yr$ (-30µm to +30µm) is applied to the closed-loop. Fig. 17.a presents the results and shows the good tracking of the output $y$. In Fig. 17.b is presented the corresponding control voltage which shows its relatively low values (< ±30V). Finally Fig. 17.c zoom a single step response of the closed-loop. In this figure is shown a good control accuracy (static error tends towards zero) and a settling time <30ms. These experimental results demonstrate the efficiency of the method used to synthesize a controller for PMN-PT actuators.

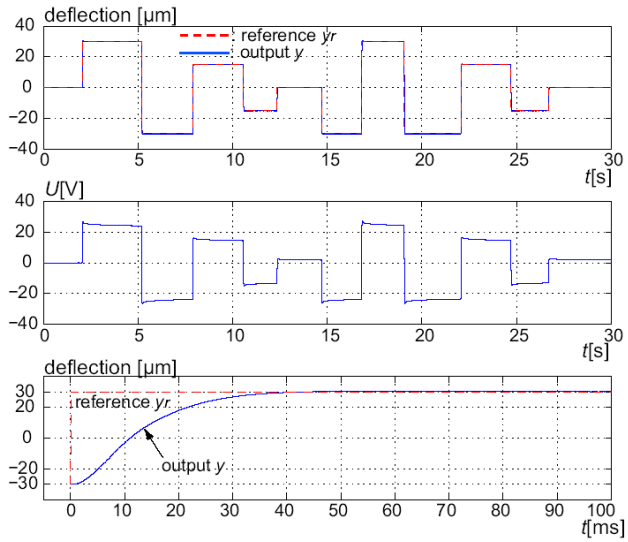


Fig. 17. Experimental results for the closed-loop. a) reference and measured displacement signals, b) the voltage control signal and c) zoomed image

## V. Conclusion

A new panel of PMN-PT on Silicon bending actuators were successfully designed, micromanufactured, tested and controlled. In fact the designed actuators exhibit an even larger actuation range than some simulation results. Compared to some PZT on Nickel cantilevers, the actuation is significantly improved, by a factor of 3 to 4, the bandwidth is improved for a faster actuation and the temperature drifts are small. The inherent drawbacks refer to a nonlinear behavior at large fields, small reverse coercitive fields and reduced Curie temperature. The external re-poling is possible and reversible, although the strain lobes are not completely symmetrical.

PMN-PT-on-Silicon actuators present some other major advantages: the sizes and/or the applied voltage levels may be reduced, all by keeping the actuation capabilities unchanged. The crystalline structure of the PMN-PT allows its etching into micrometer-size features as recently presented in [10]. In the future, thanks to the presented technique, the piezoelectric element and its related driving and/or sensing electronics will achieve new levels of integration.

## References


[1] S. Tadigadapa and K. Mateti, "*Piezoelectric MEMS sensors:state-of-the-art and perspectives*", Meas. Sci. Technol. 20 092001 (30pp), 2009

[2] X. Jiang,P. W. Rehrig, W. S. Hackenberger, E. Smith, S. Dong, D. Viehland, J. Moore, B. Patrick, "*Advanced Piezoelectric Single Crystal Based Actuators*", Proceedings of SPIE Vol. 5761, doi: 10.1117/12.600019, 2005

[3] J. Peng, S.T. Lau, C. Chao, J.Y. Dai, H.L.W. Chan, H.S. Luo, B.P. Zhu, Q.F. Zhou, K.K. Shung, "*PMN-PT single crystal thick films on silicon substrate for high-frequency micromachined ultrasonic transducers*", Appl Phys A (2010) 98: 233–237, 2010

[4] E.E. Aktakka, H. Kim, and K. Najafi, "*Wafer level fabrication of high performance MEMS using bonded and thinned bulk piezoelectric substrates*", IEEE Transducers, pp. 849-852, 2009

[5] Ioan Alexandru Ivan, Micky Rakotondrabe, Joël Agnus, Roger Bourquin, Nicolas Chaillet, Philippe Lutz, Jean-Claude Poncot, Roland Duffait, Olivier Bauer, "*Comparative material study between PZT ceramic and newer crystalline PMN-PT and PZN-PT materials for composite bimorph actuators*", Reviews on Advanced Materials Science (RAMS), No.1/2, Vol.24, pp.1-9, 2010 .

[6] Ioan Alexandru Ivan, Micky Rakotondrabe and Nicolas Chaillet, "*High Coupling Factor Piezoelectric Materials for Bending Actuators: Analytical and Finite Elements Modeling Results*", 2009 European COMSOL Conference, Milano Italy, 2009

[7] R. Zhang, W. Jiang, B. Jiang and W. Cao, "*Elastic, dielectric and piezoelectric coefficients of domain engineered 0.70Pb(Mg1/3Nb2/3)O3-0.30PbTiO3 single crystal*", AIP Conf. Proc. vol. 626, pp 188-197, 2002

[8] Micky Rakotondrabe, Yassine Haddab and Philippe Lutz, *'Quadrilateral modelling and robust control of a nonlinear piezoelectric cantilever'*, IEEE - Transactions on Control Systems Technology (T-CST), Vol.17, Issue 3, pp:528-539, May 2009.

[9] Sofiane Khadraoui, Micky Rakotondrabe and Philippe Lutz, *'Interval Modeling and Robust Control of Piezoelectric Microactuators'*, IEEE - Transactions on Control Systems Technology (T-CST), DOI.10.1109/TCST.2011.2116789, 2011.

[10] J. Agnus, I. A. Ivan and S. Queste, "D*ry etching of single crystal PMN-PT piezoelectric material*", IEEE MEMS Conference, ISBN 978-1-4244-9633-4, pp. 237-240, 2011